

# RSC Advances



This is an *Accepted Manuscript*, which has been through the Royal Society of Chemistry peer review process and has been accepted for publication.

*Accepted Manuscripts* are published online shortly after acceptance, before technical editing, formatting and proof reading. Using this free service, authors can make their results available to the community, in citable form, before we publish the edited article. This *Accepted Manuscript* will be replaced by the edited, formatted and paginated article as soon as this is available.

You can find more information about *Accepted Manuscripts* in the [Information for Authors](#).

Please note that technical editing may introduce minor changes to the text and/or graphics, which may alter content. The journal's standard [Terms & Conditions](#) and the [Ethical guidelines](#) still apply. In no event shall the Royal Society of Chemistry be held responsible for any errors or omissions in this *Accepted Manuscript* or any consequences arising from the use of any information it contains.

# Novel Pyridinium Oximes: Synthesis, Molecular Docking and *In vitro* Reactivation Studies

Pooja<sup>1,2</sup>, S. Aggarwal<sup>1,2</sup>, A.K. Tiwari<sup>1\*</sup>, V. Singh<sup>1</sup>, Ramendra Pratap<sup>2</sup>, Gurmeet Singh<sup>2</sup>, and Anil K Mishra<sup>1\*</sup>

<sup>5</sup> Received (in XXX, XXX) Xth XXXXXXXXX 20XX, Accepted Xth XXXXXXXXX 20XX

DOI: 10.1039/b000000x

Computational approach has been attempted for the screening of 4-pyridoxinium (4P) ring based reactivators for paraoxon inhibited AChE. The oxime molecules were designed with the common 4P skeleton and varying carbon linkers. Initially, AChE binding capability was accessed by molecular docking with PDB: 2WHP and 3ZLV, which showed important interactions with Ser298, Trp124 and Trp286. These computational results were validated by *in vitro* AChE binding assay, which showed binding affinity in the range of 10<sup>-5</sup>-90%. Finally, reactivation potency was calculated as % reactivation on paraoxon inhibited eelAChE in the concentration range of 10<sup>-5</sup>-10<sup>-7</sup> M. It was observed that introduction of aliphatic linker attached to 4-pyridoxime have high binding affinity and hence, may act as a good reactivator as compared to the aromatic pyridoximes.

**Keywords:** Pyridoxime, AChE, Reactivation, Paraoxon.

## 15 Introduction

Acetylcholinesterase (AChE) is a very important enzyme for the hydrolysis of neurotransmitter acetylcholine at the cholinergic synaptic site. It has two binding sites, first is active site known as A-site and second is peripheral anionic site known as PAS or P-site. Hydrolysis of acetylcholine takes place via hydrolyzing the serine residue by the active site of AChE enzyme (Scheme 1).<sup>1-6</sup> The major inhibitors of AChE are nerve gas agents which include different classes of organophosphorus (OP) compounds which bind with the -OH of the serine residue and blocks the action of AChE towards the hydrolysis of ACh into choline and acetic acid.<sup>7-9</sup> This blockage by these OP agents responsible for the high level of ACh at the cholinergic sites leads to failure of the neurotransmission process and can cause various neurological diseases of the CNS. A majorly of known OP agents are sarin, soman, tabun, VX and paraoxon (Figure 1). To inhibit the action of OP agents and to reactivate OP-inhibited AChE, various pyridoxime derivatives (Figure 2) were synthesized and reported in literature e.g., 2-PAM, HI-6 and obidoxime.<sup>10-13</sup> Pyridoxime derivatives have substitution (hydroxoiminomethyl) at their 2, 3 or 4 positions. They may interact at the active site and break the covalent bond formed between the OP agents and -OH of the serine residue of OP-inhibited AChE. 4-pyridoxime derivatives were observed to have high potency to act as reactivators of OP-inhibited AChE as compared to 2 and 3 pyridoximes. It was also observed that the positive charge on the nitrogen of the pyridoxime ring makes it more potent for reactivation but it increases hydrophilicity of the oxime moiety making it less lipophilic to cross the blood brain barrier (BBB), which is the most important lipoidal membrane. Therefore, various modifications have been done and different non-ionic oxime derivatives were reported in the literature, but it was found that they have less reactivation potency, as compared to ionic oximes. This implies that the positive charge on pyridoxime ring is important. Furthermore, carbon chain linker was introduced at the -N position of pyridoxime derivatives to give lipophilicity to the

molecule for enhancing its permeability. The studied chain with the 4-pyridoxime are alkyl, alkoxy, and aromatic carbon chains.<sup>14,15</sup> It was found that as the carbon chain length increases, lipophilicity and permeability to cross BBB increases and % reactivation towards the OP-inhibited AChE also increases. The 4-pyridoxime derivatives have higher lipophilicity when compared with 2-PAM, e.g., 30% for 4-octyl-PAM.<sup>1</sup>

These oximes have been studied on the species like rodents, which are similar to human.<sup>16</sup> We used eelAChE due to the easy and readily availability, which is one of the most explored species in preliminary studies. Though other studies have been also performed previously, to show variation in the binding and reactivation potency of oximes with different species.<sup>17-19</sup>

Here, we report the synthesis of six 4-pyridoxime derivatives having aliphatic and aromatic carbon chain linker attached at the nitrogen (-N) of the pyridoxime moiety. These derivatives were selected on the basis of preliminary computational studies and comparison with the previously synthesized oxime derivatives. Finally, *in vitro* AChE binding and reactivation study was performed to see the efficacy of these molecules for further applications.

## 2. Experimental

### 2.1 Chemicals

4-pyridine carboxaldehyde, hydroxylamine hydrochloride, 1,3-dibromo propane, 1-bromo butyrl chloride, 4-bromomethyl phenyl acetic acid, 2-bromomethyl naphthalene, N-(2-bromoethyl) phthalimide, 2-bromo acetophenone, paraoxon, eel acetylcholinesterase (eelAChE) enzyme, acetylthiocholine iodide, (DTNB), purchased from Sigma-Aldrich Co, USA. Thin layer chromatography on aluminum plates coated with silica gel 1160, F<sub>254</sub>, CHCl<sub>3</sub>, acetone, isopropanol, sodium monophosphate, and sodium diphosphate purchased from Merck, Germany.

Six different oximes were synthesized on the basis of preliminary computational prediction which are presented in figure 3. The synthetic schemes are shown as scheme 2 and 3.

## 2.2 Synthesis of Pyridine-4-carbaldehyde oxime (4P)

A solution of hydroxylamine hydrochloride (9.34 mmol, 650 mg) in water was stirred on a magnetic stirrer. The pH of the reaction mixture was maintained at 6-7 throughout the reaction by using 1 M NaOH solution.<sup>20</sup> Aqueous solution of 4-pyridine carbaldehyde (4.67 mmol, 0.44 mL) was added dropwise. Reaction mixture was kept on heating at 50 °C for 12 h. After that solvent was evaporated on rota evaporator and final product was dried under vacuum.

## 2.3 Synthesis of 1-(3-Bromo-propyl)-4-(hydroxyimino-methyl)-pyridinium (4BPB)

Pyridoxinium ion was synthesized by using 4-pyridoxime (2.03 mmol, 250 mg) in dried  $\text{CHCl}_3$  and 1, 3-dibromo propane (10.15 mmol, 1.18 mL) in  $\text{CHCl}_3$ .<sup>21</sup> This reaction mixture was stirred first at room temperature for 10 min after that allowed at reflux condition of temperature 60 °C for 72 h. White precipitate was appeared in the reaction mixture, which was filtered and dried under vacuum.

## 2.4 Synthesis of 1-(4-Bromo-butyryl)-4-(hydroxyimino-methyl)-pyridinium (4PBB)

4PBB was synthesised similar to the procedure for 4BPB by adding 4-bromo butyryl chloride (2.23 mmol, 0.28 mL) in  $\text{CHCl}_3$  in place of 1,3-dibromo propane. Reaction mixture was stirred at room temperature for 1 h after that white precipitates appeared in the reaction mixture. It was filtered and solvent was evaporated under vacuum on rota evaporator.

## 2.5 Synthesis of 1-(4-Carboxymethyl-benzyl)-4-(hydroxyimino-methyl)-pyridinium (4PCB)

4PCB was synthesised by the reaction between 4-pyridoxime (2.03 mmol, 250 mg) in dried acetone and 4-(bromo methyl) phenyl acetic acid (3.65 mmol, 1.680 gm).<sup>22</sup> Reaction mixture was stirred at refluxing for 28 h after that precipitates appeared in the reaction mixture. It was filtered and solvent was evaporated under vacuum on rota evaporator.

## 2.6 Synthesis of 4-(hydroxyimino-methyl)-1-(2-oxo-2-phenylethyl)-pyridinium (4OA)

In a two neck round bottom flask, reaction of 4-pyridoxime (1.00 mmol, 124 mg) with 2-bromoacetophenone (2.50 mmol, 497.6 mg) was added in dry acetone. Reflux conditions were maintained for 15 h. The progress of the reaction was checked using TLC.

## 2.7 Synthesis of 4-(hydroxyimino-methyl)-1-naphthalen-2-ylmethyl-pyridinium (4ON)

Synthesis of '4-(hydroxyimino-methyl)-1-naphthalen-2-ylmethyl-pyridinium' (4ON) was carried out by a substitution reaction of 4-pyridoxime with bromo-functionalized naphthalene moiety. 4-Pyridoxime (1.00 mmol, 123.7 mg) was added in a two neck round bottom flask and dissolved in dry acetone. Then 2-bromomethylnaphthalene (2.50 mmol, 552.7 mg) was added to the reaction mixture and stirring at reflux was continued for 15 h. The TLC was monitored at regular intervals.

## 2.8 Synthesis of 1-[2-(1,3-dioxo-1,3-dihydro-isoindol-2-yl)-ethyl]-4-(hydroxyimino-methyl)-pyridinium (4OPh)

To a solution of 4-pyridoxime (1.00 mmol, 123.7 mg) in dry acetone, N-(2-bromoethyl) phthalimide (2.50 mmol, 635.2 mg) was added. The reaction mixture was kept at stirring under reflux conditions for 15 h and the completion of the reaction was checked by TLC.

## 2.9 Computational Approach for AChE interaction

The X-ray crystal structure of sarinphosphonylated (PDB entry 2WHP, having resolution of 2.20 Å)<sup>23</sup> and tabuncomplexed acetylcholinesterase (PDB entry 3ZLV, having resolution of 2.50 Å)<sup>24</sup> were used for molecular docking studies. The following criteria were kept in mind before choosing the protein-ligand complexes: non-covalent binding between protein and ligand, crystallographic resolution less than or equal to 2.5 Å and known experimental binding data. Molecular modeling investigations were carried out using an advanced molecular docking program GLIDE, 5.8.<sup>25</sup> During the docking process, initially GLIDE performs a complete systematic search of the conformational, orientation and positional space of the docked ligand eliminating unwanted conformations using scoring followed by energy optimization. Preparation of the protein for docking included removal of unnecessary heteroatom and solvent coupled with addition of hydrogen atoms, bond order for crystal ligand and protein were adjusted and minimized up to 0.30 Å RMSD.

## 2.10 Binding Study with AChE

Mixture of 750 µL enzyme (eelAChE, 0.1 mg in 20 mL sodium phosphate buffer of pH 7.4), 750 µL acetylthiocholine iodide as a substrate (550 µM) and 750 µL oxime solution in the range of concentration 1 mM to 1 nM was incubated for 12 h at 25 °C. A parallel experiment was running in which 750 µL buffer was used in place of test compound in the enzyme solution as a positive control. In each concentration sample 750 µL DTNB solution (80 µM, prepared in phosphate buffer of pH 7.4) was added and absorbance was recorded at 412 nm at every 5 min for 30 min.<sup>26,27</sup>

Enzyme activity was calculated by using the formula:

$$\% \text{ AChE activity} = \frac{A_i}{A_o} \times 100$$

Where,  $A_o$  and  $A_i$  are the absorbance for the positive control and test compound respectively.

## 2.11 Reactivation Study towards Paraoxon Inhibited AChE

To study the reactivation on inhibited AChE, the foremost necessity was to know about the inhibited enzyme activity. So, 30 µL enzyme was incubated with 10 µL paraoxon ( $10^{-2}$ - $10^{-5}$  M) for 15 min to achieve >95% inhibition. Thereafter, a mixture of 40 µL inhibited enzyme, 40 µL acetylthiocholine iodide and 40 µL PBS buffer was incubated for 15 min. Then, absorbance ( $A_i$ ) was measured at 412 nm by adding 40 µL DTNB at different time intervals, 0 min, 15 min, 30 min, 45 min and 60 min.

For reactivation study, a mixture of 40 µL inhibited enzyme, 40 µL acetylthiocholine iodide and 40 µL test oxime ( $10^{-3}$ - $10^{-8}$  M) was incubated for 15 min and absorbance ( $A_r$ ) was recorded at

412 nm by adding 40  $\mu\text{L}$  DTNB at different time interval. A parallel positive control experiment was done by taking 40  $\mu\text{L}$  enzyme and 40  $\mu\text{L}$  buffer in place of inhibited enzyme and test oxime respectively.<sup>1,15,26</sup>

% AChE reactivation was calculated by using the formula:

$$\% \text{AChE reactivation} = (A_r - A_i / A_o - A_i) \times 100$$

Where,  $A_r$ ,  $A_i$  and  $A_o$  are the absorbance of test oxime, inhibited enzyme and positive control found experimentally.

## 2.12 Fluorometric Assay with Human Serum Albumin (HSA)

Binding constant of the oximes with HSA was calculated by the fluorometric experiments. The fluorescence intensity was recorded at  $\lambda_{em}=350$  nm at the fixed  $\lambda_{ex}=280$  nm for the different concentration of oximes from  $4 \times 10^{-4}$  to  $10^{-5}$  M in PBS of pH=7.4 at 25 °C while the concentration of HSA was fixed at  $2 \times 10^{-5}$  M. The change in intensity at 350 nm (tryptophan) was used to calculate the binding constant (K).<sup>28,29</sup> The binding constant was calculated by the Stern-Volmer equation<sup>30</sup>:

$$\frac{F_0}{F} = 1 + K_{sv}[Q]$$

Where  $F_0$  and  $F$  denotes the fluorescence intensity in the absence and presence of quencher pyridoxime, respectively.  $K_{sv}$  is the Stern-Volmer quenching constant (or binding constant) and  $[Q]$  is the concentration of quencher.

## 3. Result and Discussion

### 3.1 Synthesis of 4P

4-pyridoxime was synthesized by the hydrolysis reaction between 4-pyridine carbaldehyde and hydroxylamine as shown in Scheme 2. The product was obtained in high yield of 97.17% by evaporating solvent and its structure was confirmed by <sup>1</sup>H NMR, <sup>13</sup>C NMR and mass spectroscopy (shown as S1).

<sup>1</sup>H NMR (400 MHz, DMSO):  $\delta=7.5$  (d, 2H, ArH), 8.1 (d, 1H, -CH proton), 8.5 (d, 2H, ArH), <sup>13</sup>C NMR (100 MHz, DMSO):  $\delta=120.94$  (ArC), 141.05 (ArC), 146.73 (ArC), 150.68 (-CH=NOH), m/z (ESI-LCMS): Calculated mass  $[M^+]=122.05$ ,  $[M+H^+]=123.4$ .

### 3.2 Synthesis of 4PBP

N-(3-Bromo-propyl)-4-pyridoxime was synthesized by the N-alkylation reaction between 4-pyridoxime and 1,3-dibromopropane as Shown in Scheme 2. The product was obtained as brown precipitate with moderate yield of 60.34% and its structure was confirmed by <sup>1</sup>H NMR, <sup>13</sup>C NMR and mass spectroscopy (shown as S2).

<sup>1</sup>H NMR (400 MHz, D<sub>2</sub>O):  $\delta=8.75$  (d, 2H, ArH), 8.66 (s, 1H, ArH), 8.25 (d, 2H, ArH), 4.65 (s, D<sub>2</sub>O), 3.43 (t, 2H, -CH<sub>2</sub>), 2.66 (t, 2H, -CH<sub>2</sub>), 2.14 (m, 2H, -CH<sub>2</sub>), <sup>13</sup>C NMR (100 MHz, D<sub>2</sub>O):  $\delta=149.19$  (-CH=NOH), 146.23 (ArC), 144.62 (ArC), 125.13 (ArC), 57.70, 32.61, 31.58, m/z (ESI-LCMS): Calculated mass  $[M^+]=243.01$ ,  $[M+H^+]=244.9$ , with M: (M+2):1:1 bromo isotopic pattern.

### 3.3 Synthesis of 4PBB

N-Alkylation reaction between 4-pyridoxime and 4-bromo butyryl chloride yields N-(4-bromo-butyryl)-4-pyridoxime with 59.24% as shown in Scheme 2. Its structure was confirmed by <sup>1</sup>H NMR, <sup>13</sup>C NMR and mass spectroscopy (shown as S3).

<sup>1</sup>H NMR (400 MHz, D<sub>2</sub>O):  $\delta=8.74$  (d, 2H, ArH), 8.66 (s, 1H, ArH), 8.59 (d, 2H, ArH), 4.65 (s, D<sub>2</sub>O), 3.42 (t, 2H, -CH<sub>2</sub>), 2.66 (t, 2H, -CH<sub>2</sub>), 2.41 (m, 2H, -CH<sub>2</sub>), <sup>13</sup>C NMR (100 MHz, D<sub>2</sub>O):  $\delta=183.22$  (-C=O), 146.78 (-CH=NOH), 141.49 (ArC), 130.47 (ArC), 124.17 (ArC), 30.33, 27.94, 26.48, m/z (ESI-LCMS): Calculated mass  $[M^+]=271$ ,  $[M+H^+]=271.3$ , with M: (M+2):1:1 bromo isotopic pattern.

### 3.4 Synthesis of 4PCB

N-Alkylation between 4-pyridoxime and 4-bromo methyl phenyl acetic acid gives N-(4-carboxymethyl-benzyl)-4-pyridoxime in the form of yellow colored compound as shown in Scheme 2. 78.45% yield was obtained and structure confirmation was done by <sup>1</sup>H NMR, <sup>13</sup>C NMR and mass spectroscopy (shown as S4).

<sup>1</sup>H NMR (400 MHz, D<sub>2</sub>O):  $\delta=8.70$  (d, 2H, ArH), 8.19 (s, 1H, -CH), 8.01 (d, 2H, ArH), 7.22-7.31 (dd, 4H, ArH), 5.62 (s, 2H, -CH<sub>2</sub>), 4.65 (s, D<sub>2</sub>O peak), 3.59 (s, 2H, -CH<sub>2</sub>), <sup>13</sup>C NMR (100 MHz, D<sub>2</sub>O):  $\delta=176.63$  (-COOH), 148.93 (-CH=NOH), 146.22, 144.48, 136.23, 131.58, 130.65, 129.48, 124.91 (ArC's), 63.86, 40.39, m/z (ESI-LCMS): Calculated mass  $[M^+]=271.11$ ,  $[M^+]=271.3$ ,  $[M+Na^+]=294$ .

### 3.5 Synthesis of 4OA

4-(hydroxyimino-methyl)-1-(2-oxo-2-phenyl-ethyl)-pyridinium was synthesized by the N-alkylation reaction between 4-pyridoxime and 2-bromoacetophenone as shown in Scheme 3. The product was obtained by evaporating solvent as a white powder in moderate yield of 72.01% and its structure has been confirmed by <sup>1</sup>H NMR, <sup>13</sup>C NMR and mass spectroscopy (shown as S5).

<sup>1</sup>H NMR (CDCl<sub>3</sub>, 400 MHz):  $\delta$  values (ppm) = 4.19 (s, 2H, CH<sub>2</sub>), 7.51-7.69 (m, 3H, ArH), 7.94-7.96 (d, 2H, ArH), 8.04-8.07 (m, 1H, ArH) 8.25 (s, 1H, CH=N), 8.69-8.71 (d, 2H, ArH), 8.88 (s, 1H, ArH). <sup>13</sup>C NMR (CDCl<sub>3</sub>, 100 MHz):  $\delta$  values (ppm) = 60.4 (CH<sub>2</sub>), 114.6 (ArCH), 128.1 (ArCH), 128.5 (ArCH), 129.5 (ArCH), 132.7 (ArCH), 133.6 (ArCH), 135.8 (ArCH), 143.3 (ArCH), 143.9 (ArC), 144.6 (ArC), 145.8 (CH), 192.1 (C=O). ESI-MS: m/z =241.2  $[M]^+$ .

### 3.6 Synthesis of 4ON

4-(hydroxyimino-methyl)-1-naphthalen-2-ylmethyl-pyridinium was synthesized by the N-alkylation reaction between 4-pyridoxime and 2-bromomethylnaphthalene as shown in Scheme 3. The product was obtained by evaporating solvent as a pale yellow powder in moderate yield of 65.12% and its structure has been confirmed by <sup>1</sup>H NMR, <sup>13</sup>C NMR and mass spectroscopy (shown as S6).

<sup>1</sup>H NMR (CDCl<sub>3</sub>, 400 MHz):  $\delta$  values (ppm) = 2.91 (s, 2H, CH<sub>2</sub>), 7.27-7.7.81 (m, 7H, ArH), 8.17-8.19 (d, 2H, ArH), 8.45 (s, 1H, CH=N), 8.91-8.93 (d, 2H, ArH). <sup>13</sup>C NMR (CDCl<sub>3</sub>, 100 MHz):  $\delta$

values (ppm) = 64.3 (CH<sub>2</sub>), 124.7 (ArCH), 125.5 (ArCH), 127.2 (ArCH), 127.5 (ArCH), 127.7 (ArCH), 128.1 (ArCH), 128.9 (ArCH), 129.5 (ArCH), 130.2 (ArCH), 132.8 (ArC), 133.1 (ArC), 144.3 (ArC), 146.0 (ArC), 148.7 (CH). ESI-MS: m/z =263.3 [M]<sup>+</sup>.

### 3.7 Synthesis of 4OPh

1-[2-(1,3-dioxo-1,3-dihydro-isoindol-2-yl)-ethyl]-4-(hydroxyimino-methyl)-pyridinium (1g) was synthesized by the N-alkylation reaction between 4-pyridoxime and N-(2-bromoethyl)phthalimide as shown in Scheme 3. The product was obtained by evaporating solvent as a white powder in moderate yield of 61.34% and its structure has been confirmed by <sup>1</sup>H NMR, <sup>13</sup>C NMR and mass spectroscopy (shown as S7).

<sup>1</sup>H NMR (CDCl<sub>3</sub>, 400 MHz): δ values (ppm) = 4.18-4.21 (t, 2H, CH<sub>2</sub>), 4.76-4.79 (t, 2H, CH<sub>2</sub>), 7.71-7.75 (m, 4H, ArH), 8.04-8.06 (d, 2H, ArH), 8.24 (s, 1H, CH=N), 8.75-8.77 (d, 2H, ArH). <sup>13</sup>C NMR (CDCl<sub>3</sub>, 100 MHz): δ values (ppm) = 38.3 (CH<sub>2</sub>), 59.6 (CH<sub>2</sub>), 123.7 (ArCH), 124.9 (ArCH), 130.7 (ArCH), 135.1 (ArCH), 144.9 (ArC), 146.0 (ArC), 149.4 (CH), 169.7 (C=O). ESI-MS: m/z =296.1 [M]<sup>+</sup>.

### 3.8 Computational Approach for AChE interaction

Molecular modeling studies were performed on synthesized oxime molecules 4PBP, 4PBB, 4PCB, 4OA, 4ON and 4OPh for the justification of their interaction with OP-inhibited hAChE. It is important for a reactivator of AChE to bind with the enzyme which was revealed in the form of Glide Gscore. Binding affinity of synthesized 4-pyridoximes varies by changing the alkyl chain substituted to the pyridinium nitrogen of the ring. It was observed that the Glide Gscore for aliphatic chain alkyl group attached to pyridoximes are high (-9.920, -11.021 for 4PBP and -10.793, -10.902 for 4PBB) as compared to the aromatic (-9.951, -9.760 for 4PCB, -10.250, -8.927 for 4OA, -8.639, -8.261 for 4ON and -9.202, -8.244 for 4OPh) with both the PDB's 2WHP and 3ZLV (detail shown in S8). This variation in Glide Gscores is due to difference in the type of linkers in each oxime which affect the binding with various amino acid residues. These synthesized oximes showed binding with Trp286 and Tyr124 via π-π interaction with the aromatic moiety of amino acid and pyridinium ring, which is an important interaction for oximes to reactivate nerve gas inhibited AChE.<sup>26</sup> These amino acid residues are present at peripheral anionic binding site of enzyme AChE. It is known that attack of OP on the -OH of serine residue present at the ester site is important for any reactivator to bind with the serine residue and its bond breakage was previously formed by OP agents. Oximes showed binding with Ser298 of AChE by hydroxyimino moiety via hydrogen bonding interaction, except for aromatic linker attached oximes (4OA, 4ON and 4OPh). In 4PBP and 4PBB extra interactions were observed including π-π interaction with the amino acid residue Tyr72. While, aromatic linker attached pyridoximes showed less interaction as compared to aliphatic linker due to rigidity in the structure. The 2-D diagrams of oximes with PDB 2WHP and 3ZLV were shown in figure 4 and figure 5, respectively. These results were compared with the well known AChE reactivator 2-PAM (2D interaction shown in figure 6). The reliability of the docking program Glide used in this study was verified evaluating its performances in reproducing the geometry of bound inhibitors taken from crystallized complexes (2WHP and 3ZLV). The docking calculation reproduces the actual orientation of these molecules

as shown in S9. This was further validated by MD simulation and MMGBSA analysis. Furthermore, to validate this computational binding *therein vitro* binding and reactivation potency were studied towards OP-inhibited AChE.

**MD simulations:** MD simulation was performed as per our previous work on same pdb.<sup>31</sup> Model system was placed inside orthorhombic box containing explicit water molecules modeled as TIP3P. Three sodium ions (Na<sup>+</sup>) ions were added to neutralize the whole system which was relaxed before simulation and energy of the system is minimized by force field OPLS2005. This is followed by submission of a system containing 55394 atoms, to MD simulation which was subsequently carried out by using following procedure: first, default 1.2ns run of MD simulation at constant temperature of 300 K and with all atoms having positions restrained except for the water molecules inside the box under the NPT ensemble. This initial MD was necessary in order to allow the equilibration of the solvent molecules around the protein. Another production run was carried out which included: full MD simulations of 5ns at 300K with no restrictions with 2fs of integration time. After completion, simulations quality and event analysis was done.

**MM-GBSA Analysis:** The MM-GBSA analysis was used to calculate ligand binding energies based on docking complex, by using the MM-GBSA technology available in Schrödinger's tool Prime (Schrödinger, LLC, New York, NY, 2013). This analysis was done by including poser viewer file of glide docked complexes and by assuming the default parameters in the panel. The binding energy is calculated according to the equation:

$$\Delta G_{\text{bind}} = \Delta E_{\text{MM}} + \Delta G_{\text{solv}} + \Delta G_{\text{SA}}$$

Where the term  $\Delta E_{\text{MM}}$  comes from difference between minimized energies of Protein-oxime complexes and individual minimized energies of protein and Oxime.  $\Delta G_{\text{solv}}$  is a difference between GBSA energies of complexed protein-oxime and unliganded 2-protein and Oxime.  $\Delta G_{\text{SA}}$  is the difference in surface area energies for the complex and the sum of the surface area energies for the protein and Oxime. The Prime's contribution of  $\Delta G_{\text{SA}}$  to the  $\Delta G_{\text{bind}}$  comes from the non-polar contribution to the solvation energy due to the surface area.

MMGBSA energy profile with 3ZLV and 2WHP are shown in S10 and S11 along with 3D interactive poses in S12 and simulation interactions for the NPT ensemble 4PBB-2WHP presented in S13 for 5ns.

### 3.9 Binding Study with AChE

An oxime can only reactivate AChE if it goes to the site of OP-inhibited AChE and bind to inhibit it. To get more insight of the reactivation of inhibited AChE, binding affinity of the synthesized oximes was evaluated with eelAChE by measuring their inhibitory activity using Ellman method. Binding experiment was performed in which eelAChE was incubated with different concentrations (10<sup>-3</sup>-10<sup>-9</sup> M) of oximes for 12 h to achieve the maximum inhibition. Binding affinity was also measured for the precursor 4-pyridoxime to compare. The *in vitro* data is shown in Figure 7. It was observed that all the synthesized oximes showed change in binding affinity by changing the concentration. Out of six synthesized oximes, 4PBB and 4PCB showed highest binding affinity. At the concentrations 10<sup>-9</sup>-10<sup>-7</sup> M, 4PBP have less inhibitory activity as compared to 4PBB and

4PCB. But at the concentrations  $10^{-6}$ ,  $10^{-4}$  and  $10^{-3}$  M it showed inhibitory activity of 1%, 1% and 50% for 4BPB, 15%, 80% and 95% for 4PBB, 40%, 92% and 60% for 4PCB, 36%, 29% and 74% for 4OA, 44%, 45% and 52% for 4ON, 30%, 87% and 89% for 4OPh and 10%, 40% and 60% for precursor 4P respectively. It was also observed that at the biological concentration of  $10^{-9}$ ,  $10^{-8}$  and  $10^{-7}$  M these oximes do not show much efficient inhibitory activity as compared to the concentration of  $10^{-6}$ ,  $10^{-4}$  and  $10^{-3}$  M. They showed optimum inhibitory activity at the concentration range of  $10^{-4}$  M.

### 3.10 Reactivation Study towards Paraoxon Inhibited AChE

To validate the binding affinity of synthesized pyridoximes with AChE, *in vitro* reactivation experiment was demonstrated with the paraoxon inhibited eel-AChE.<sup>10</sup> Enzyme was incubated with the nerve gas paraoxon about 30 min to achieve maximum inhibition. Then enzyme activity was determined by performing well known Ellman assay<sup>27</sup> using DTNB as a coloring agent. This assay was performed on the synthesized pyridoximes (4BPB, 4PBB, 4PCB, 4OA, 4ON and 4OPh) as well as with the synthesized precursor 4P. These reactivation potencies were also compared with the currently used AChE reactivator 2-PAM. The results of reactivation experiment were shown in figure 8, which showed reactivation % by varying the concentration of pyridoximes.

This experiment showed that the reactivation potency of the oximes varied by changing the linker at the pyridinium nitrogen of the ring. It was observed that the reactivation potency for the synthesized oximes 4BPB and 4PBB were high as compared to the aromatic ring bearing pyridoximes (4PCB, 4OA, 4ON and 4OPh). Results showed 61.82%, 89.09%, 76.36% reactivation potency for 4BPB, 76.36%, 65.45%, 81.82% for 4PBB, -32.73%, 32.73%, 21.82% for 4PCB, -0.04%, -0.19%, -0.03% for 4OA, 3.00%, 5.00%, -1.00% for 4ON and -0.04%, 0.02%, -0.02% for 4OPh at the concentration of  $10^{-5}$  M,  $10^{-6}$  M and  $10^{-7}$  M respectively. These results were also compared with the precursor 4P which showed reactivation potency 56.36%, 49.09%, 56.36% for the same concentration range as for the products. Reactivation potency was evaluated for the known reactivator 2-PAM which showed 16.39%, 9.18%, 2.30% reactivation at the concentration  $10^{-5}$  M,  $10^{-6}$  M and  $10^{-7}$  M respectively. For the aromatic ring bearing pyridoximes, reactivation was also studied at high concentration of  $10^{-3}$  M and  $10^{-4}$  M. It was found that these oximes able to reactivate paraoxon inhibited AChE at high concentrations with the % reactivation of, 22.73%, 36.36% for 4PCB at  $10^{-3}$  M and  $10^{-4}$  M, 20.00%, for 4OA at  $10^{-3}$  M, 49.51%, 42.95% for 4ON at  $10^{-3}$  M and  $10^{-4}$  M and 42.95%, 15.08% for 4OPh at  $10^{-3}$  M and  $10^{-4}$  M respectively. This data stated as we move from aliphatic to aromatic linker, reactivation potency decreases and also the synthesized oximes showed high reactivation potency at low concentration range between  $10^{-6}$ - $10^{-7}$  M. Secondly, these data showed better reactivation than known reactivator 2-PAM. In 2-PAM, oxime group was at 2nd position of the pyridinium ring while it was at 4th position in our synthesized oximes. Synthesized oxime precursor 4P is also more effective than the 2-PAM at low concentrations.

Reactivation potency for 2-PAM decreased as the concentration decreases which showed that they are good reactivators at the high concentration but not at the low concentration. Both the aliphatic chain linked with pyridoximes, 4BPB and 4PBB showed similar reactivation potencies, but if observed at each

concentration then it was found that 4PBB have good reactivation potency (81.82%) at the concentration  $10^{-7}$  M whereas 4BPB showed excellent reactivation potency (89.09%) at  $10^{-6}$  M.

### 3.11 HSA Binding Assay

Interaction of ligand with HSA was analyzed by *in vitro* fluorometric assay. HSA shows emission because of aromatic amino acids tryptophan, tyrosine and phenylalanine residues present in it. Quenching of fluorescence intensity of tyrosine was observed if it is present near an amino, a carboxyl group or a tryptophan, and phenylalanine with very low quantum yield. Small molecules bound to HSA tend to change in intrinsic fluorescence intensity due to tryptophan residue in the oxime system. Hence, fluorescence quenching was observed by addition of oxime in the concentration range of 0.4-0.05 mM to the fixed concentration of HSA (0.02 mM) at 350 nm (figure 9 (a-d)). This quenching indicates the formation of ligand-HSA complex which leads to microenvironment change in the protein and hence showed decrease in fluorescence intensity.

The binding constants of the synthesized oximes as well as precursor 4P were calculated by Stern-Volmer plot and these data were shown in figure 10. Stern-Volmer binding constants were calculated as  $1.17 \times 10^3 \text{ M}^{-1}$ ,  $2.29 \times 10^3 \text{ M}^{-1}$ ,  $0.90 \times 10^3 \text{ M}^{-1}$  and  $0.75 \times 10^3 \text{ M}^{-1}$  for 4P, 4PBB, 4BPB and 4PCB respectively. These binding constant values suggested that the newly synthesized oximes have ability to bind with HSA for their transportation at the specific site in the body to reactivate inhibited AChE.

### 4. Conclusion

In this study mono-quaternary oximes were synthesized as reactivator for paraoxon inhibited eelAChE by variation in the carbon chain attached with the -N position of 4-pyridoxime moiety. These oximes were studied for their binding affinity with eelAChE. Further, this binding was validated with the molecular modeling studies on the basis of Glide Gscore,  $\pi$ - $\pi$  interaction and hydrophobic interaction on the active site of AChE. These synthesized oximes were found to be effective reactivators towards the paraoxon inhibited eelAChE as compared to the known reactivator 2-PAM. 4PBB and 4BPB have high reactivation potency as compared to 4PCB. Furthermore, they also showed drug likeliness behavior by showing effective pharmacokinetics properties with human serum albumin.

### Acknowledgement

We thank Dr R. P. Tripathi, Director, INMAS, DRDO for providing the necessary facilities and CSIR for financial assistance to the first and second authors during the course of the research work.

### Notes and references

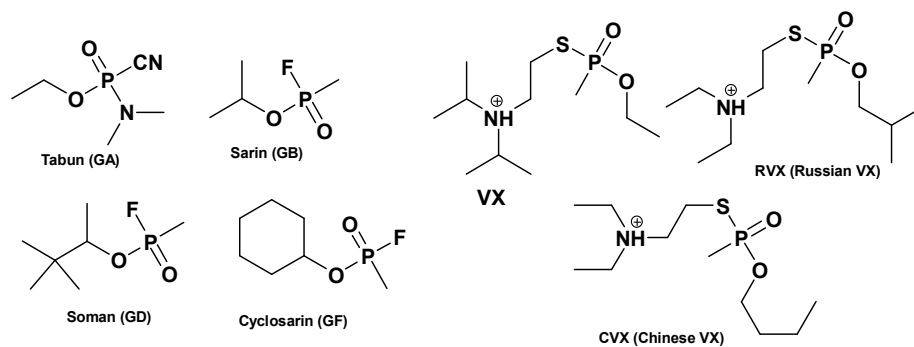
<sup>1</sup> Division of Cyclotron and Radiopharmaceutical Sciences, Institute of Nuclear Medicine and Allied Sciences, Brig. S. K. Mazumdar Road, Delhi-110054, India, \*[anjani7797@rediffmail.com](mailto:anjani7797@rediffmail.com),  
<sup>110</sup> \*[akmishra63@gmail.com](mailto:akmishra63@gmail.com)

<sup>2</sup> Department of Chemistry, University of Delhi, Delhi-110054, India.

† Electronic Supplementary Information (ESI) available: [supplementary information contains associated figures and tables]. See DOI: 10.1039/b000000x/.

- [1] M. C. De Koning, M. J. A. Joosen, D. Noort, A. Van Zuylen, M. C. Tromp, *Bioorg. Med. Chem.*, 2011, 19, 588-594.
- [2] Z. Kovarik, N. Macek, R. K. Sit, Z. Radic, V. V. Fokin, K. B. Sharpless, P. Taylor, *Chem. Biol. Interact.*, 2013, 203, 77-80.
- [3] T. H. Kim, K. Kuca, D. Jun, Y. S. Jung, *Bioorg. Med. Chem. Lett.*, 2005, 15, 2914-2917.
- [4] K. Musilek, K. Kuca, D. Jun, V. Dohnal, M. Dolezal, *Bioorg. Med. Chem. Lett.*, 2006, 16, 622-627.
- [5] K. Musilek, O. Holas, K. Kuca, D. Jun, V. Dohnal, M. Dolezal, *Bioorg. Med. Chem. Lett.*, 2006, 16, 5673-5676.
- [6] K. Musilek, J. Roder, M. KomLoova, O. Holas, M. Hbinova, M. Pohanka, V. Dohnal, V. Opletalova, K. Kuca, Y. S. Jung, *Bioorg. Med. Chem. Lett.*, 2011, 21, 150-154.
- [7] S. B. Bharate, L. Guo, T. E. Reeves, D. M. Cerasoli, C. M. Thompson, *Bioorg. Med. Chem.*, 2010, 18, 787-794.
- [8] J. Acharya, A. K. Gupta, A. Mazumder, D. K. Dubey, *Toxicol. In Vitro*, 2008, 22, 525-530.
- [9] G. Sinko, J. Brglez, Z. Kovarik, *Chem. Biol. Interact.*, 2010, 187, 172-176.
- [10] S. B. Bharate, L. Guo, T. E. Reeves, D. M. Cerasoli, C. M. Thompson, *Bioorg. Med. Chem. Lett.*, 2009, 19, 5101-5104.
- [11] K. Musilek, O. Holas, D. Jun, V. Dohnal, F. G. Moore, V. Opletalova, M. Dolezal, K. Kuca, *Bioorg. Med. Chem.*, 2007, 15, 6733-6741.
- [12] K. Kuca, J. Bielavsky, J. Cabal, M. Bielavska, *Tetrahedron Lett.* 2003, 44, 3123-3125.
- [13] F. Ekstrom, J. C. Astot, Y. P. Pang, *Clin. Pharmacol. Ther.*, 2007, 82, 282-293.
- [14] A. Luettringhaus, I. Hagedorn, *Arzneimittelforschung*, 1964, 14, 1-5.
- [15] J. Acharya, D. K. Dubey, A. K. Srivastava, S. K. Raza, *Toxicol. In Vitro*, 2011, 25, 251-256.
- [16] J. J. Kassa, *Toxicol. Clin. Toxicol.* 2002, 40, 803-816.
- [17] F. Worek, G. Reiter, P. Eyer, L. Szinicz, *Arch. Toxicol.*, 2002, 76, 523-529.
- [18] J. G. Clement, N. Erhardt, *Arch. Toxicol.*, 1994, 68, 648-659.
- [19] W. K. Berry, *Biochem. Pharmacol.* 1971, 20, 1333-1334.
- [20] X. Q. Feng, Z. S. Zeng, Y. H. Liang, F. E. Chen, C. Pannecouque, J. Balzarini, E. D. Clercq, *Bioorg. Med. Chem.*, 2010, 18, 2370-2374.
- [21] S. R. Chennamaneni, V. Vobalaboina, A. Garlapati, *Bioorg. Med. Chem. Lett.*, 2005, 15, 3076-3080.
- [22] A. K. Sikder, A. K. Ghosh, D. K. Jaiswal, *Journal of Pharmaceutical Sciences*, 1993, 82, 258-261.
- [23] F. Ekstrom, A. Hornberg, E. Artursson, L. G. Hammarstrom, G. Schneider, Y. P. Pang, *Plos one*, 2009, 4, 59-57.
- [24] E. Artursson, P. O. Andersson, C. Akfur, A. Linusson, S. Borjegen, F. Ekstrom, *Biochem. Pharmacol.* 2013, 85, 1389-1397.
- [25] R. A. Friesner, R. B. Murphy, M. P. Repasky, L. L. Frye, J. R. Greenwood, T. A. Halgren, P. C. Sanschagrin, and D. T. Mainz, *J. Med. Chem.*, 2006, 49, 6177-6196.
- [26] K. Musilek, M. KomLoova, O. Holas, A. Horova, M. Pohanka, F. G. Moore, V. Dohnal, M. Dolezal, K. Kuca, *Bioorg. Med. Chem.*, 2011, 19, 754-762.
- [27] G. L. Ellman, D. K. Courtney, V. Andreas, R. M. Featherstone, *Biochem. Pharmacol.*, 1961, 7, 88-95.
- [28] H. H. Sun, J. Zhang, Y. Z. Zhang, L. Y. Yang, L. L. Yuan, Y. Liu, *Mol. Biol. Rep.*, 2012, 39, 5115-5123.
- [29] P. Bourassa, S. Dubeau, G. M. Maharvi, A. H. Fauq, T. J. Thomas, H. A. T. Riahi, *Biochimie.*, 2011, 93, 1089-1101.
- [30] H. X. Zhang, P. Mei, *J. Solut. Chem.*, 2009, 38, 351-355.
- [31] N. Chadha, A.K.Tiwari, V.Kumar, S. Lal, M.D.Milton, A.K.Mishra. *J Biomol Struct Dyn.* 2014, 29, 1-13.

## FIGURES:

**Figure 1:** Organophosphorus (OP) as Nerve agents

5

10

**Figure 2:** Representative Pyridoxime derivatives as AChE reactivators

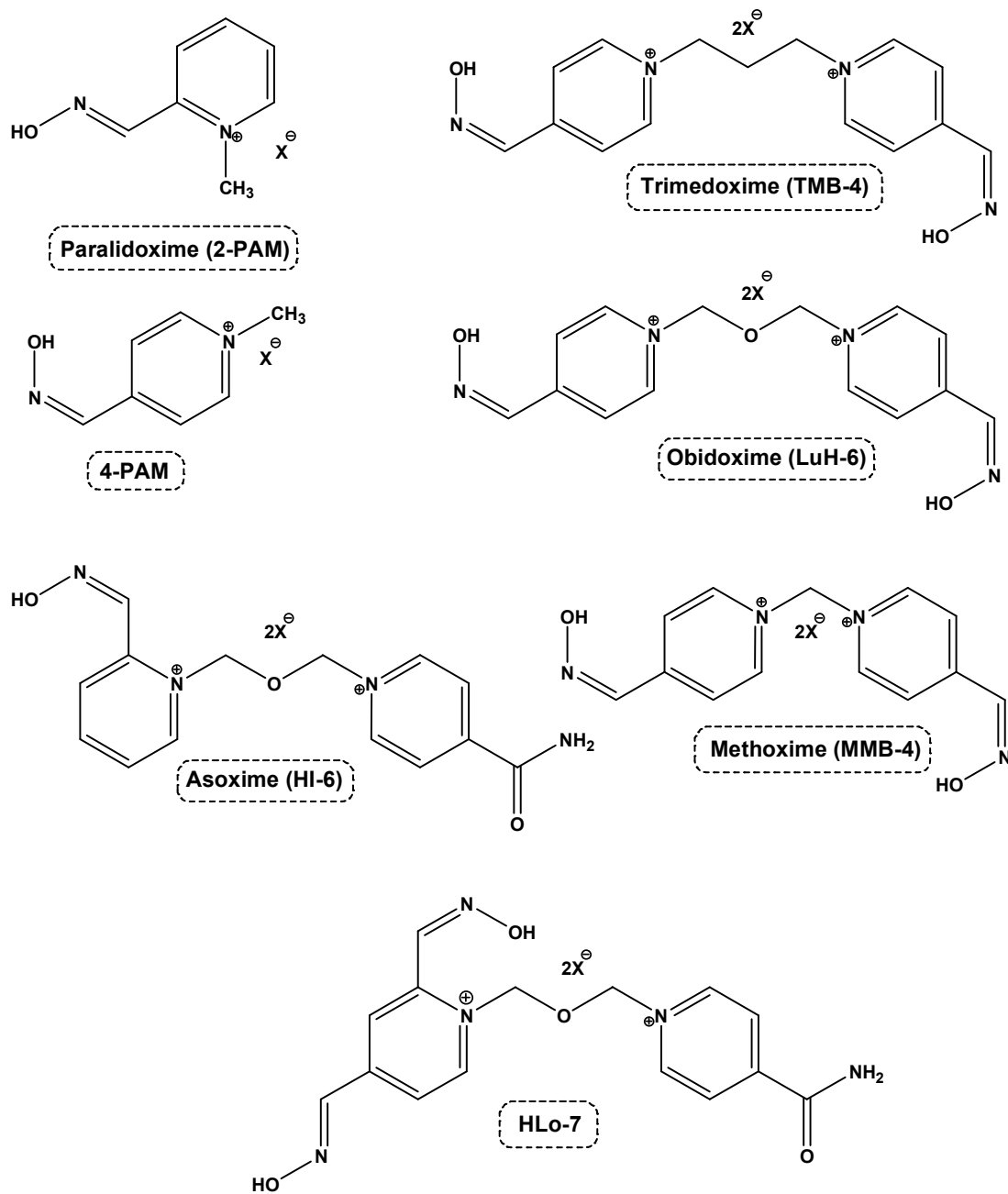
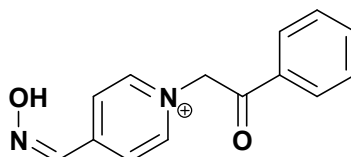
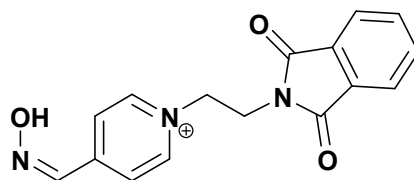
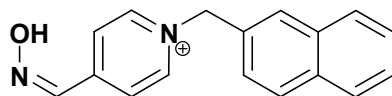
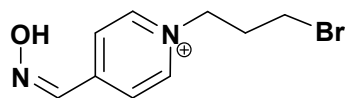
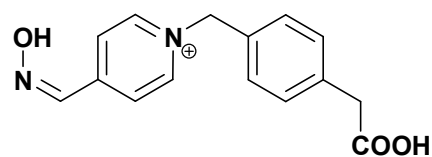
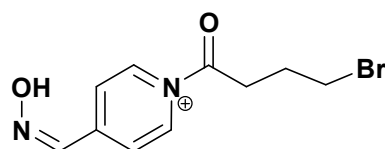


**Figure 3:** Structures of newly developed oxime reactivators

5



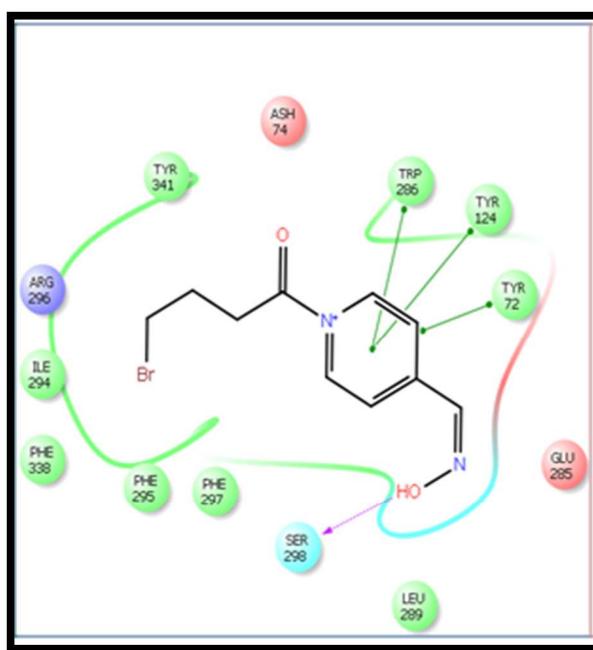
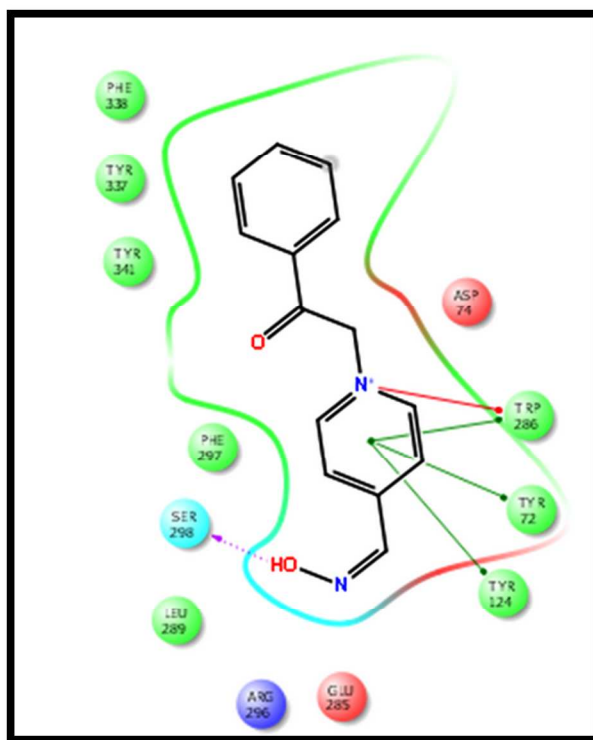
[a]

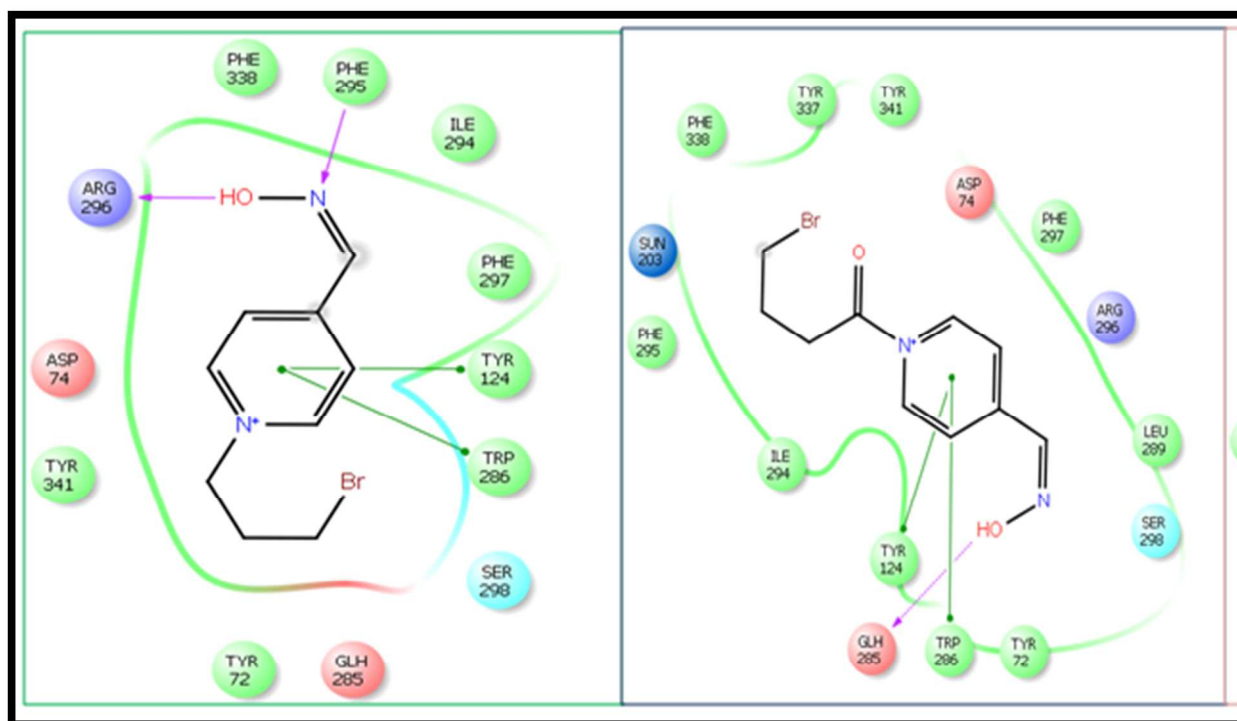


[b]

s # [a]4OA, 4ON, 4OPh

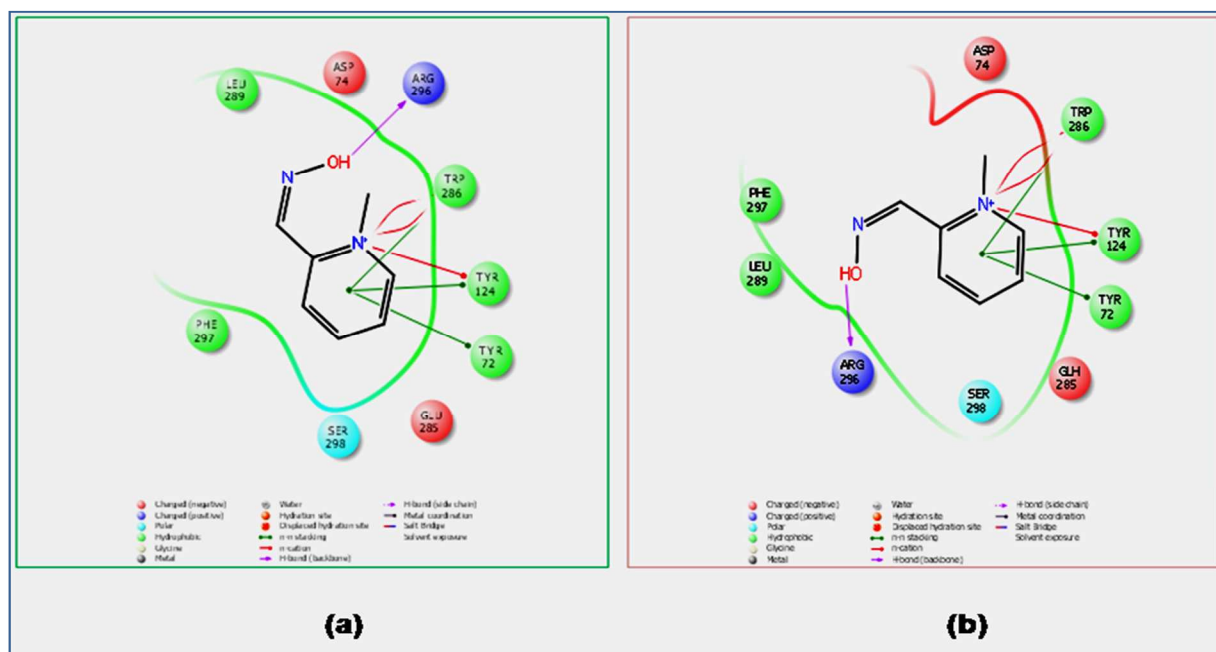
[b] 4PBP, 4PBB, 4PCB

**Figure 4:** 2D interaction diagrams for synthesized oximes with 2WHP (a) 4PB (b) 4OA

**Figure 5:** 2D interaction diagrams for synthesized oximes with 3ZLV (a) 4PBP (b) 4PBB

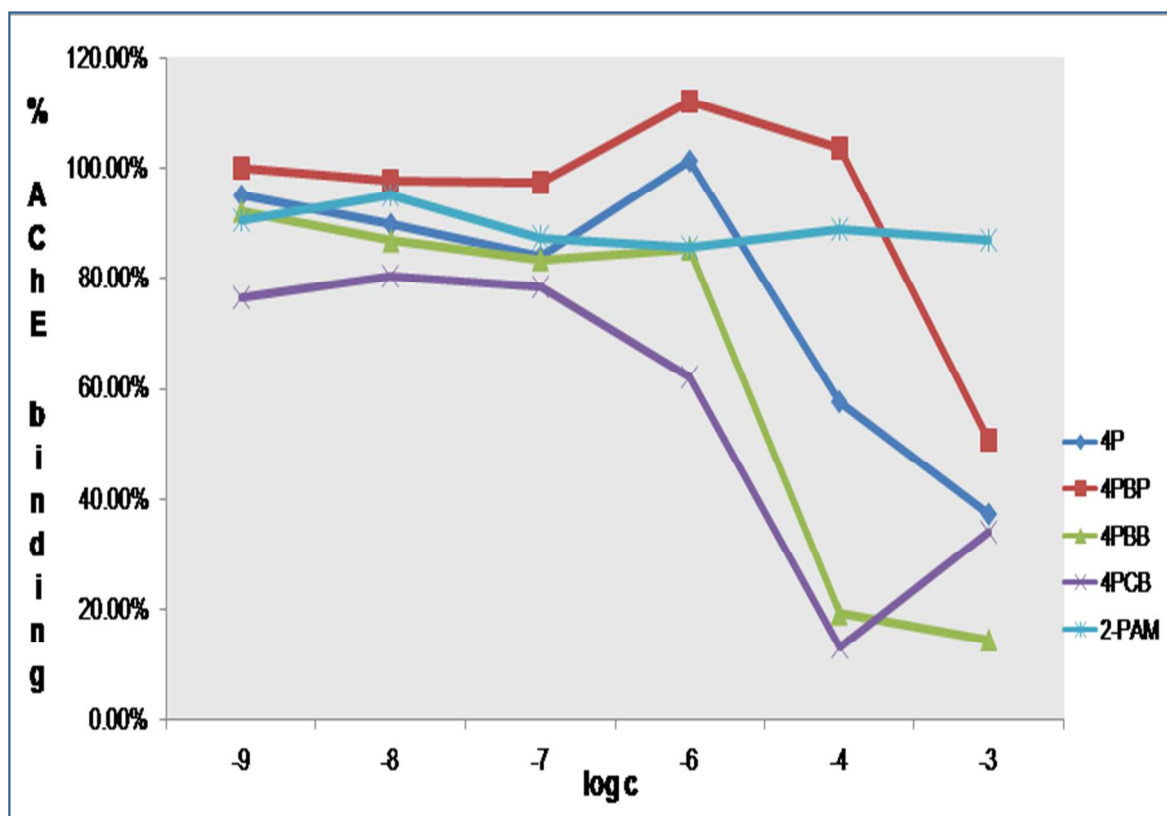
5

10

**Figure 6:** 2D interaction diagrams for known AChE reactivator 2-PAM with (a) 2WHP (b) 3ZLV

5

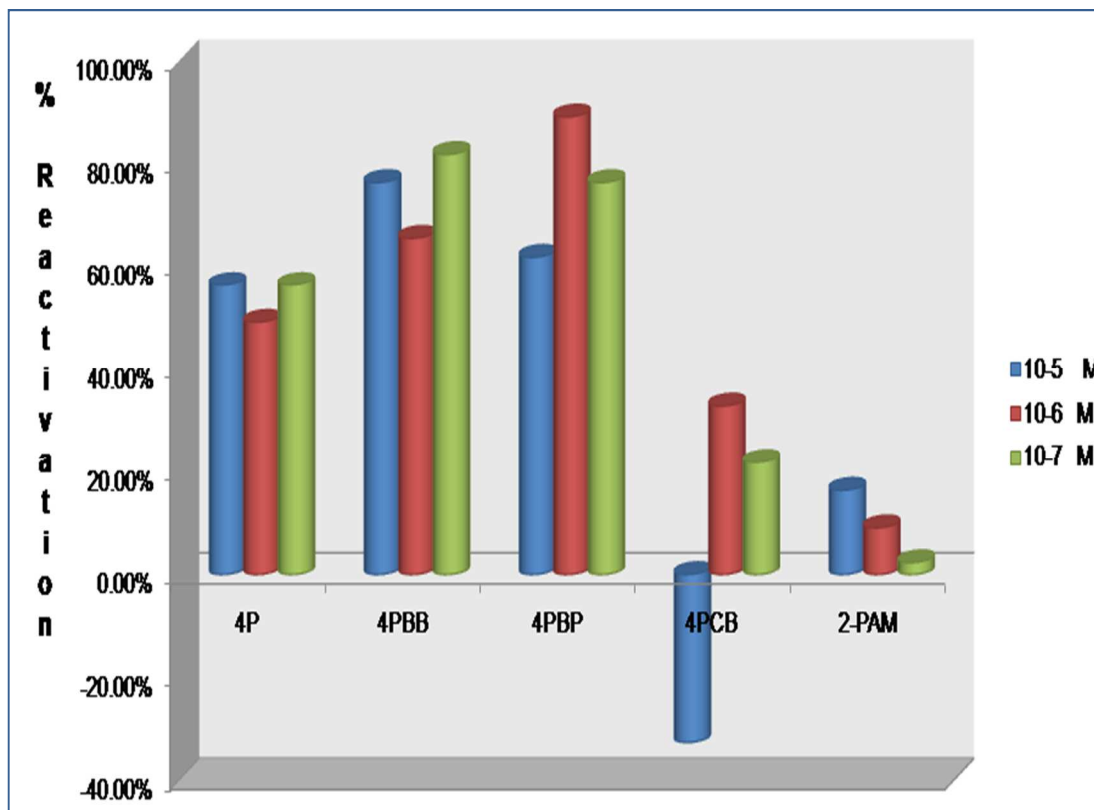
10

**Figure 7:** Binding affinity of eelAChE with oximes and 2-PAM at varying concentration

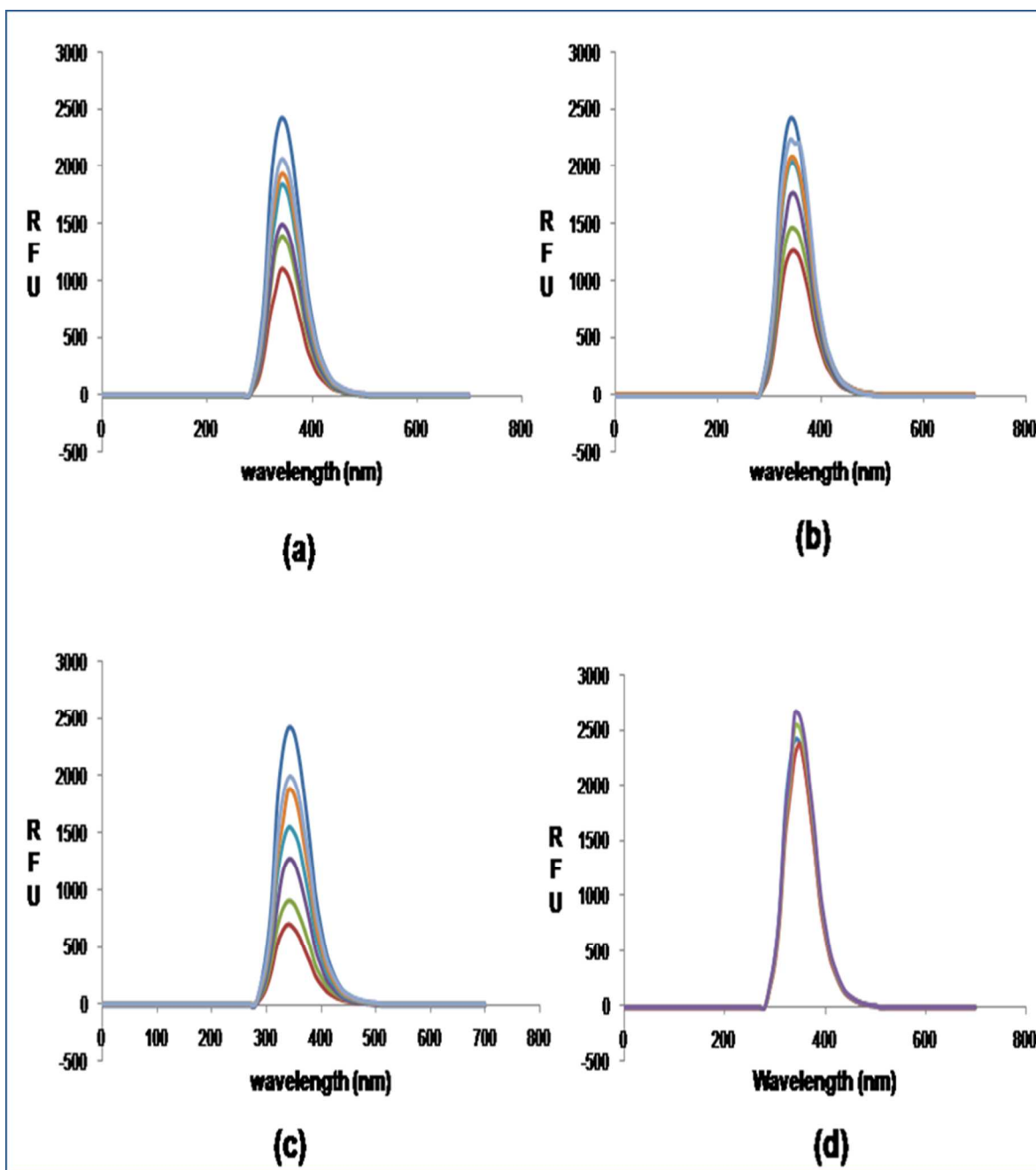
Binding experiment was performed in eelAChE, which was incubated with different concentrations ( $10^{-3}$ – $10^{-9}$  M) of oximes for 12 h to achieve the maximum inhibition.

5 Binding affinity was also measured for the precursor 4-pyridoxime for the comparison purpose and positive control was taken by replacing oxime with buffer.

**Figure 8:** Reactivation of paraoxon inhibited eelAChE by oximes and 2-PAM at different concentrations



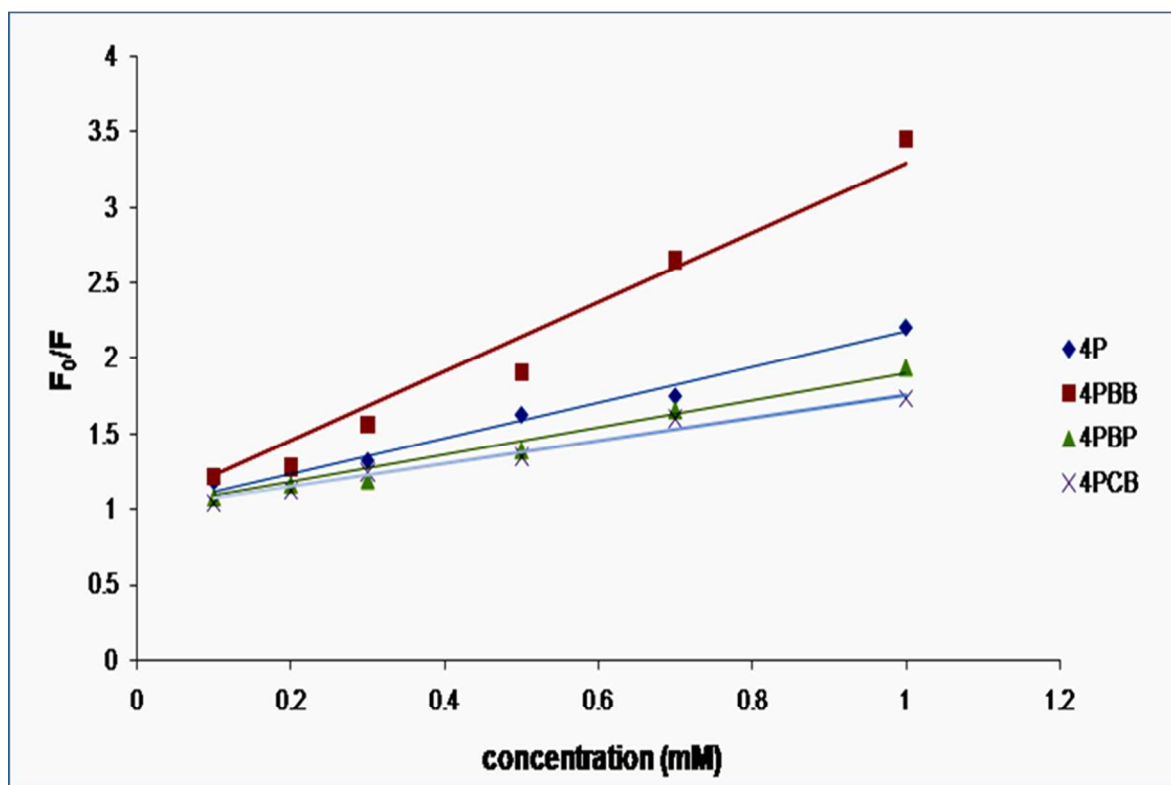
Reactivation efficacy (%) of the oximes in comparison to 2-PAM at 60 min against paraoxon inhibited *eelAChE* (three concentration of oximes, 0.1 M phosphate buffer, pH 7.4 and temperature 37 °C).

**Figure 9:** Emission plot for ligand-HSA fluorescence quenching with different oximes

# (a) 4P (b) 4PBP (c) 4PBB (d) 4PCB

5

**Figure 10:** Stern-Volmer plot for for determination of the binding constantt of the oxime-HSA

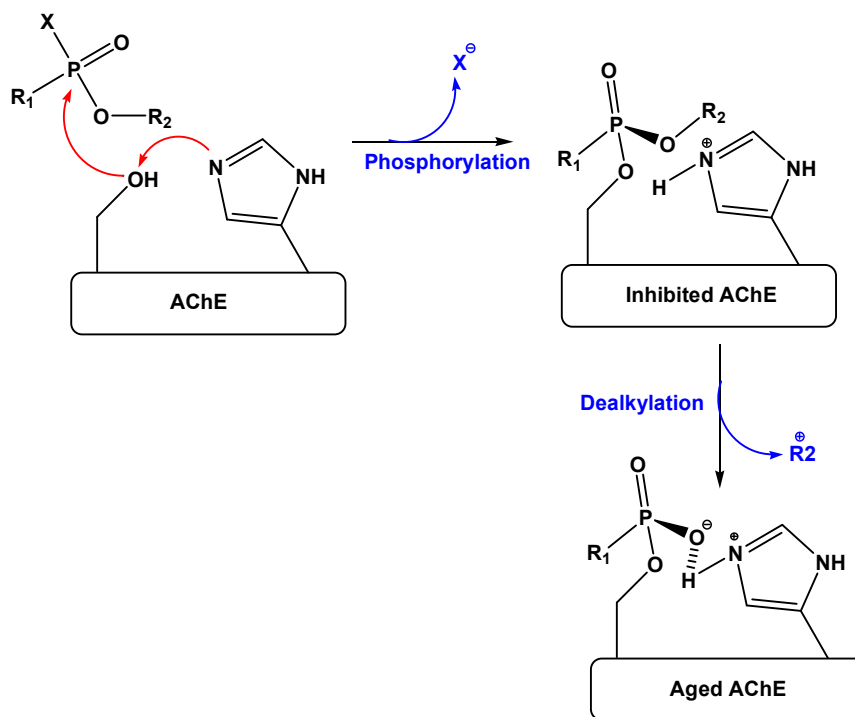


5

10

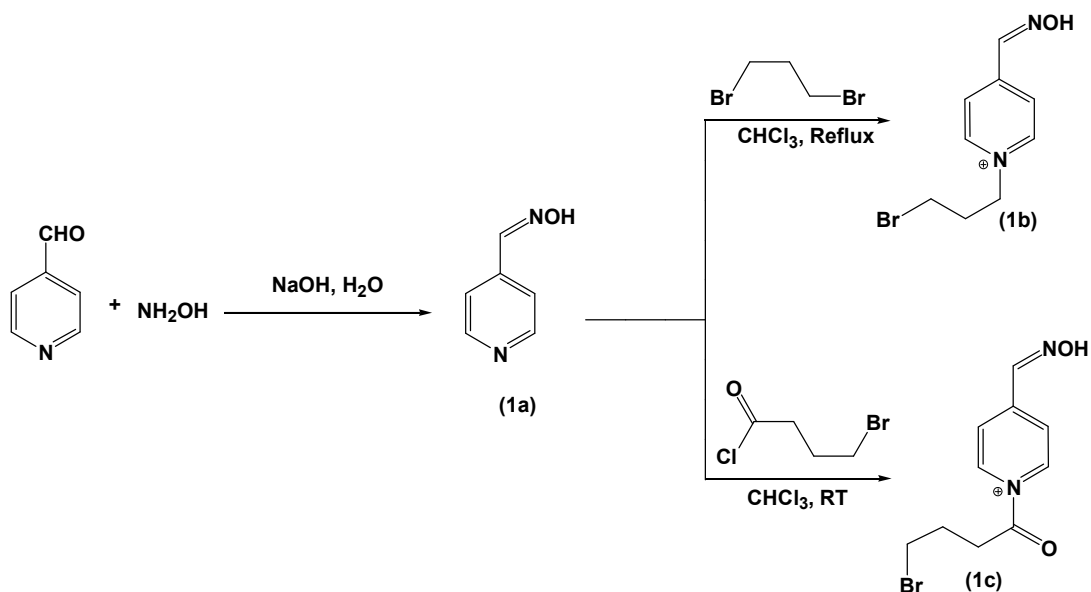
## SCHEMES:

Scheme 1: Mechanism of AChE inhibition by OP agents.



5

Scheme 2: Synthetic scheme for monoquaternary aliphatic linker oximes



Scheme 3: Synthetic scheme for monoquaternary aromatic linker oximes

